

# Identifiability in Blind Source Separation through Stabilizer Shrinkage: Unifying Non-Gaussianity and Observation Diversity

Tomomi Ogawa and Hiroki Matsumoto

**Abstract**—Identifiability is a central issue in blind source separation (BSS), determining whether latent sources can be uniquely recovered from observed mixtures. Classical approaches address identifiability either by exploiting source non-Gaussianity via higher-order statistics (HOS) or by enriching the observation structure through temporal, spatial, or multi-channel diversity using second-order statistics (SOS), and these routes are often regarded as fundamentally different. In this paper, we revisit identifiability in BSS from a structural perspective, interpreting it as constraint-induced reduction of residual ambiguity in the mixing model. Within this framework, the observation mechanism is viewed broadly to include both input-side statistical constraints and output-side observation structures. HOS-based and SOS-based approaches are then unified as mechanisms of *stabilizer shrinkage*, in which observation-induced constraints reduce an initially continuous ambiguity to a finite residual one. To connect this structural viewpoint with finite-sample regimes, we introduce a Jacobian-based sensitivity probe as a numerical diagnostic of local identifiability. Numerical experiments show that increasing non-Gaussianity or observation diversity suppresses the same residual symmetry, revealing a structural trade-off between source statistics and observation design. These results provide a unified interpretation of classical BSS methods and clarify how observation constraints govern identifiability.

**Index Terms**—Blind source separation, identifiability, stabilizer, higher-order statistics, second-order statistics, observation diversity.

## I. INTRODUCTION

Blind source separation (BSS) aims to recover latent source signals from observed mixtures without prior knowledge of the mixing process, and identifiability lies at the core of this task [1]. Even when separation algorithms converge and standard performance indices appear satisfactory, residual ambiguities may remain [2]. Such ambiguities reflect intrinsic limitations of the observation mechanism rather than algorithmic failure. Clarifying when and why they can or cannot be eliminated is therefore essential for interpreting classical BSS methods and for guiding the design of new ones.

Classical studies of identifiability in BSS have largely followed two complementary routes [3]–[6]. Higher-order statistics (HOS)–based methods exploit deviations from Gaussianity to impose distributional constraints that are not accessible through second-order analysis [7]. In contrast, second-order statistics (SOS)–based methods enrich the observation

structure via temporal, spatial, or multi-channel diversity, thereby imposing multiple correlation-based constraints [2], [8]. Throughout this paper, we use the term *multi-SOS* to refer to second-order statistics constructed from multiple lags or blocks (e.g., delayed covariance matrices in SOBI-type methods), in contrast to single-lag second-order statistics. These two routes are commonly regarded as fundamentally different, resulting in distinct algorithmic families and design heuristics. Consequently, identifiability has typically been discussed either from the standpoint of source statistics or from that of observation diversity, with limited conceptual integration between the two.

Recent data-driven and deep learning–based approaches further complicate this landscape [9], [10]. Although such methods often achieve strong empirical performance, they do not directly address the structural question of identifiability: to what extent does the observation mechanism itself resolve ambiguity, independently of model capacity or training data? This question motivates a structural treatment of identifiability based on how observations constrain admissible transformations of the mixing model [11].

From this perspective, identifiability is not viewed as an algorithmic outcome but as a property of the observation mechanism itself. Specifically, it depends on whether observation-induced constraints reduce an initially continuous ambiguity to a finite residual one. In the sequel, this idea is formalized by introducing an observation-induced equivalence relation in Section II, characterizing the associated stabilizer of admissible transformations in Section IV, and examining its local manifestation through Jacobian sensitivity in Section V.

Within this framework, observation statistics are interpreted as invariance constraints on the mixing matrix, and residual ambiguities correspond to transformations that preserve all enforced statistics. Identifiability is therefore characterized by the extent to which these constraints restrict the admissible transformation group. In particular, HOS-based approaches impose constraints primarily on the *input side* through assumptions on source statistics such as non-Gaussianity and independence, whereas multi-SOS-based approaches impose constraints on the *output side* by enriching the observation structure through temporal, spatial, or multi-channel diversity in second-order statistics. Both classes of methods can thus be interpreted as mechanisms that reduce residual ambiguity by shrinking the stabilizer of the mixing model. This structural reduction, termed *stabilizer shrinkage* and formalized in Section IV-C, provides a unified viewpoint in which distributional information and observation diversity act as alternative sources

Tomomi Ogawa is with the Graduate School of Science and Engineering, Tokyo Denki University, Saitama, Japan (e-mail: to.ogawa@mail.dendai.ac.jp).

Hiroki Matsumoto is with the Graduate School of Engineering, Maebashi Institute of Technology, Gumma, Japan (e-mail: matsumoto@maebashi-it.ac.jp).

of constraint richness for ambiguity reduction.

An immediate implication of this viewpoint is that observation mechanisms producing identical stabilizer shrinkage necessarily yield identical local identifiability properties, regardless of whether the constraints arise from HOS or from multi-SOS statistics. Differences between algorithms therefore reflect how stabilizer-reducing constraints are instantiated rather than fundamentally distinct identifiability principles.

To connect this structural analysis to finite-sample regimes, we introduce a Jacobian-based sensitivity probe as a numerical diagnostic of local identifiability. The probe is used strictly as a measurement tool, not as a new identifiability criterion, to assess how strongly observation constraints suppress weakly observable perturbation directions. Because the Jacobian captures the first-order response of the observation map, its nullspace reflects residual stabilizer directions, enabling diagnostic comparison of different constraint configurations even when global identifiability conditions are formally satisfied.

Controlled numerical experiments illustrate that (i) HOS constraints strengthen identifiability as non-Gaussianity increases, (ii) multi-lag SOS constraints recover identifiability through observation diversity even under Gaussian sources, and (iii) the trade-off between these mechanisms can be visualized within a common structural framework.

The main contributions of this paper are summarized as follows:

- A structural interpretation of identifiability in BSS based on constraint-induced ambiguity reduction, independent of specific separation algorithms.
- A unified framework of stabilizer shrinkage that relates HOS-based and SOS-based approaches and clarifies their complementary roles.
- A Jacobian-based sensitivity probe as a practical diagnostic tool for visualizing local identifiability under finite-sample conditions.
- Numerical experiments illustrating how non-Gaussianity and observation diversity contribute to ambiguity reduction within a common structural probe.

The remainder of the paper is organized as follows. Section II introduces the problem formulation and inherent ambiguities. Section III reviews classical HOS-based and SOS-based approaches from a constraint-oriented perspective. Section IV develops the structural viewpoint on observation-induced constraints and symmetry. Section V formalizes local identifiability via Jacobian sensitivity. Section VI examines the relationship between non-Gaussianity and observation diversity, and Section VII presents numerical experiments validating the proposed interpretation. Section VIII concludes the paper and discusses implications for the design and diagnosis of observation constraints in blind source separation. Appendix A provides the formal definition of the Jacobian-based probe, while Appendix B summarizes representative counterexamples in which observation-induced constraints fail to reduce ambiguity.

## II. PROBLEM FORMULATION AND NOTATION

### A. Blind Source Separation Model

We begin by fixing the basic blind source separation (BSS) model and the associated equivalence class, which serve as the reference throughout the paper.

We consider the standard linear instantaneous BSS model [1], [12]

$$x(t) = Hs(t), \quad (1)$$

where  $s(t) \in \mathbb{R}^n$  denotes statistically independent source signals and  $H \in \mathbb{R}^{m \times n}$  is an unknown mixing matrix. The objective of BSS is to recover the source signals, or an equivalent representation thereof, solely from the observed mixtures  $x(t)$ , without prior knowledge of  $H$ .

Throughout this paper, we focus on square or overdetermined mixtures ( $m \geq n$ ), and consider both real-valued and complex-valued formulations, as they naturally arise in applications such as audio signal processing and communication systems [13]. No specific algorithmic structure is assumed at this stage; the analysis is intended to be independent of particular separation methods [7].

When second-order statistics are involved, we assume that the observations are whitened using the sample covariance [3], [4]. Here, for a zero-mean vector process  $v(t)$ , we define  $\text{Cov}(v) := \mathbb{E}[v(t)v(t)^\top]$  (or  $\mathbb{E}[v(t)v(t)^*]$  in the complex-valued case), where  $\mathbb{E}[\cdot]$  denotes statistical expectation,  $(\cdot)^\top$  the transpose, and  $(\cdot)^*$  the conjugate transpose.

Under the linear model (1), the covariance of the observations satisfies

$$\text{Cov}(x) = H \text{Cov}(s) H^\top. \quad (2)$$

In practice, whitening is achieved by a linear transformation  $W$  such that

$$\text{Cov}(Wx) = I, \quad (3)$$

where  $I$  denotes the identity matrix of appropriate dimension. Under (1), this implies that the effective mixing matrix  $WH$  satisfies  $(WH)(WH)^\top = I$  in the real-valued case (or  $(WH)(WH)^* = I$  in the complex-valued case), and can therefore be regarded as orthogonal (or unitary). In the following, we adopt the common convention of absorbing the whitening transform into the observation, and reuse the symbol  $x$  to denote the whitened signal.

Accordingly, without loss of generality, the mixing matrix can be considered up to a residual right-orthogonal (or unitary) transformation. Specifically, one may assume that after whitening,

$$\text{Cov}(x) = I \implies H \sim HQ, \quad (4)$$

where the symbol  $\sim$  denotes an equivalence relation on the set of mixing matrices, identifying representations that differ only by a residual right-orthogonal (or unitary) transformation. The residual transformation  $Q$  satisfies

$$Q \in \begin{cases} \mathcal{O}(n), & \text{real-valued case,} \\ \mathcal{U}(n), & \text{complex-valued case,} \end{cases} \quad (5)$$

reflecting the fact that whitening fixes the zero-lag covariance up to an orthogonal or unitary change of basis. Here,  $\mathcal{O}(n)$  and

$\mathcal{U}(n)$  denote the orthogonal and unitary groups of dimension  $n$ , respectively, with dimensions consistent with the whitened model. The symbol  $I$  should not be confused with the index set  $\mathcal{I}$  used later to label observation constraints.

This preprocessing does not alter identifiability in the sense considered here. Rather, it isolates the residual ambiguities to orthogonal (or unitary) transformations, a property that plays a central role in the subsequent analysis.

It is well known that, even under ideal conditions, the BSS problem does not admit a unique solution. Instead, recovered sources are determined only up to inherent ambiguities. In particular, demixing solutions related by permutation and component-wise scaling (or phase rotations in the complex-valued case) are indistinguishable from the observations [3]. Accordingly, throughout this paper we regard two mixing matrices as equivalent if

$$H \sim HPD, \quad (6)$$

where  $P$  is a permutation matrix and  $D$  is a nonsingular diagonal matrix (representing scaling or phase factors). This equivalence relation fixes the notion of identifiability considered in the sequel.

### B. Ambiguities and Equivalence up to Inherent Transformations

A fundamental characteristic of blind source separation is that its solutions are not unique, even in the absence of noise and estimation errors. This non-uniqueness does not arise from algorithmic imperfections, but is intrinsic to the BSS model itself [2], [14]. Specifically, certain transformations applied to the recovered sources produce alternative solutions that remain consistent with the observed mixtures.

In practice, the inherent ambiguities described by (6) include permutations of the source order and component-wise scaling, or phase rotations in the complex-valued case. Such transformations preserve the validity of the separation in the sense that they lead to reconstructed sources compatible with the observed data, despite differences in parameter representation. Throughout this paper, equivalence is understood strictly in this BSS-specific sense. At this stage, no additional algebraic or group-theoretic structure is assumed; the purpose of this subsection is solely to clarify which ambiguities are considered inherent to the model.

This perspective is essential for interpreting identifiability in blind source separation. Rather than asking whether a unique parameter estimate exists, the relevant question is which ambiguities can or cannot be resolved by the available information [15]. Identifiability is therefore determined by the extent to which observation-derived constraints restrict the equivalence class (6) [2].

In the following subsection, this viewpoint is formalized by examining how different classes of observation statistics act as constraints that progressively limit the set of admissible transformations.

### C. Observation Statistics as Constraint-Inducing Information

Throughout this paper, identifiability is considered up to the *finite* inherent ambiguities described in Section II-B (per-

mutation and component-wise scaling, or phase rotations in the complex-valued case). After whitening (Section II-A), these finite ambiguities are preceded by a *continuous* right-orthogonal (or unitary) freedom, reflecting the fact that second-order statistics alone cannot distinguish right-unitary reparameterizations of the mixing matrix. The general linear group  $\text{GL}(n)$  is introduced here as a convenient parametrization of admissible reparameterizations of the mixing matrix *before* observation-induced constraints are imposed; after whitening, the relevant residual transformations reduce locally to right-orthogonal (or unitary) actions as discussed in Section II-A.

In blind source separation, the only information available for resolving these ambiguities arises from statistical properties of the observed signals. We therefore interpret observation statistics structurally, as constraints imposed by the observation mechanism itself, which restrict admissible transformations of the mixing matrix while remaining consistent with the observed data.

To formalize this viewpoint, we introduce an observation map

$$\Phi : H \mapsto \{A_i(H)\}_{i \in \mathcal{I}}, \quad (7)$$

where each  $A_i(H)$  is a matrix-valued quantity induced by a chosen class of observation statistics. The index set  $\mathcal{I}$  specifies which statistical constraints are imposed simultaneously. Typical examples include higher-order cumulant matrices in HOS-based approaches or covariance-based operators in SOS-based approaches [5], [16]. Each operator  $A_i(H)$  is defined by applying a fixed, predetermined construction rule (e.g., a population cumulant or covariance operator) to the model  $x(t) = Hs(t)$ ; the same construction rule is applied when evaluating  $A_i(HG)$  for any admissible transformation  $G$ . For example, in the HOS case  $A_i(H)$  may correspond to population fourth-order cumulant matrices, whereas in the SOS case it may represent lagged covariance operators evaluated at different lags.

For clarity, the term *multi-SOS* is used to collectively refer to second-order constraint families involving multiple operators, including but not limited to lagged covariance matrices, multi-sensor or multi-channel observations, block or oversampled covariance structures, and covariance operators obtained under multiple experimental conditions [5], [17], [18]. In this usage, specific instances such as *multi-lag SOS* correspond to concrete realizations based on temporal lag diversity. In contrast, the labels *HOS-based* and *SOS-based* are used when emphasizing the type of statistics being exploited, whereas the term *multi-SOS* highlights the structural level at which multiple second-order operators jointly impose constraints.

The collection  $\{A_i(H)\}_{i \in \mathcal{I}}$  represents invariants of the observation: any admissible transformation of  $H$  must preserve all of these quantities. Specifically, a transformation  $G \in \text{GL}(n)$  is said to be compatible with the observation if

$$A_i(HG) = A_i(H), \quad \forall i \in \mathcal{I}. \quad (8)$$

This invariance condition can be equivalently rewritten as

$$A_i(HG) = A_i(H) \forall i \iff \Phi(HG) = \Phi(H), \quad (9)$$

which makes explicit that admissible transformations are those that leave the observation map unchanged.

Accordingly, we define the residual ambiguity set induced by the observation map  $\Phi$  as

$$\text{Stab}(\mathcal{I}) \triangleq \{G \in \text{GL}(n) \mid A_i(HG) = A_i(H), \forall i \in \mathcal{I}\}. \quad (10)$$

The terminology ‘‘stabilizer’’ is used here in the standard sense of group actions, referring to the subgroup of transformations that leave a given object invariant (see, e.g., [19]).

The set  $\text{Stab}(\mathcal{I})$  captures the remaining symmetries of the mixing matrix that cannot be resolved from the available statistics. In practice, different choices of observation statistics lead to different *degrees of stabilizer reduction*: while whitening alone leaves a continuous right-unitary stabilizer, appropriately chosen and sufficiently rich observation constraints can, under well-understood conditions, reduce this continuous ambiguity to a *finite* residual group. In this sense, identifiability is governed by how strongly the observation map  $\Phi$  restricts admissible transformations of  $H$ , rather than by the numerical procedure used to estimate it.

*Remark on identifiability:* Identifiability in blind source separation does not arise from output non-Gaussianity alone, nor from structural richness of the input process when such structure is not fixed by the observation operators. Instead, identifiability emerges only when source-side constraints (e.g., non-Gaussianity combined with independence) or output-side operator diversity effectively reduce the continuous right-unitary freedom to a finite residual ambiguity. Formal counterexamples illustrating these asymmetries are summarized in Appendix B.

#### D. Scope and Assumptions

The scope of this paper is deliberately restricted in order to focus on the structural aspects of identifiability in blind source separation. Specifically, we consider linear instantaneous mixture models with statistically independent sources [20], as introduced in Section II-A. This setting encompasses a broad class of classical BSS problems while allowing the effects of different observation constraints to be examined without confounding factors arising from model complexity.

The analysis primarily addresses separation methods based on second-order and higher-order observation statistics, including those exploiting temporal, spatial, or multi-observation diversity. No assumptions are made on a particular algorithmic implementation, and the discussion is not tied to specific optimization procedures. Instead, the emphasis is placed on how different classes of statistical information constrain the underlying model and influence the resolution of inherent ambiguities.

Several extensions of the basic BSS model are intentionally not considered [9], [10], [21]. These include nonlinear or convolutive mixtures, deep learning-based separation frameworks, and problem formulations that rely on supervised or semi-supervised training. While these settings are of practical interest, they introduce additional sources of ambiguity and inductive bias that obscure the structural effects studied here. By limiting attention to the classical linear BSS framework,

the analysis aims to isolate and clarify the role of observation-induced constraints in shaping identifiability.

### III. BACKGROUND: HOS-BASED AND SOS-BASED BLIND SOURCE SEPARATION

Blind source separation has been studied extensively under a variety of assumptions and problem settings. Among classical approaches, methods based on higher-order statistics (HOS) and those based on second-order statistics (SOS) have played a central role and are often treated as distinct methodological families. This section briefly reviews these two classes, focusing on their roles as *constraint-inducing mechanisms* rather than on algorithmic details.

#### A. HOS-Based Approaches

HOS-based approaches exploit the non-Gaussianity of source signals by introducing constraints derived from higher-order moments or cumulants, which are invisible to second-order analysis [3], [4], [7], [16], [22]–[25].

From a structural viewpoint, HOS-based methods impose constraints of the form

$$A_i(HG) = A_i(H), \quad i \in \mathcal{I}_{\text{HOS}}, \quad (11)$$

where  $A_i(H)$  denotes a matrix induced by higher-order statistics (e.g., cumulant matrices),  $G \in \text{GL}(N)$  represents an admissible transformation of the mixing matrix, and  $\mathcal{I}_{\text{HOS}}$  indexes the chosen set of HOS constraints. Equation (11) expresses the fact that only transformations preserving higher-order statistical structure remain compatible with the observation.

A key advantage of HOS-based methods is their ability to eliminate ambiguities that persist under purely second-order analysis, particularly when source distributions deviate sufficiently from Gaussianity. At the same time, the effectiveness of these constraints depends on the reliability of higher-order statistical estimation, which can be sensitive to finite-sample effects and noise.

#### B. SOS-Based Approaches

In contrast, SOS-based approaches rely on structural diversity in the observations, without assuming specific source distributions [2], [5], [6], [8], [17], [18], [26]. By exploiting multiple time lags, sensor arrays, or observation blocks, they introduce collections of second-order constraints.

A typical SOS formulation considers a collection of covariance matrices

$$R_z(\tau) = \mathbb{E}[z(t)z(t-\tau)^T], \quad \tau \in \mathcal{I}_{\text{SOS}}, \quad (12)$$

where  $z(t)$  denotes the observed (often whitened) signal, and  $\mathcal{I}_{\text{SOS}}$  specifies a set of nonzero lags or observation conditions. Each lag  $\tau$  induces a second-order constraint, and separation is achieved by enforcing joint compatibility across all selected lags.

Structurally, SOS-based methods restrict admissible transformations by requiring simultaneous consistency with multiple second-order relations. While any single covariance constraint may leave substantial ambiguity, their combination can

significantly reduce the set of transformations that preserve all imposed correlations. Such methods are often viewed as statistically robust and computationally efficient, especially in scenarios where non-Gaussianity is weak or unreliable but sufficient observation diversity is available.

### C. Structural Comparison

Although HOS-based and SOS-based methods are often presented as alternative strategies, both act by introducing additional invariance constraints that restrict admissible transformations of the mixing model. The distinction lies in the *source* of constraint information: distributional properties in the HOS case and observation diversity in the SOS case.

From the unified viewpoint developed in Section II-C, both families can be interpreted as imposing collections of invariance constraints of the form (11) or (12), which progressively restrict the set of admissible transformations compatible with the observed data. Identifiability is therefore governed by how strongly these constraints reduce the stabilizer, rather than by the statistical order or algorithmic realization.

Counterexamples in which individual constraint families fail to reduce the stabilizer are summarized in Appendix B.

## IV. STRUCTURAL VIEWPOINT: OBSERVATION CONSTRAINTS AND SYMMETRY

### A. Observation-Induced Constraints on the Mixing Model

The statistical information extracted from observed mixtures imposes structural constraints on the admissible transformations of the mixing model: only those transformations that preserve the observed statistics remain compatible with the data, while others lead to inconsistencies.

Here,  $\Phi(H) = \{A_i(H)\}_{i \in \mathcal{I}}$  refers to the observation map introduced in Section II-C. As defined in (10), the set of transformations that leave all constraint objects invariant forms the stabilizer  $\text{Stab}(\mathcal{I})$  [19]. This stabilizer represents the residual ambiguity of the mixing model under the imposed observation constraints.

When only a single class of observation statistics is enforced, the corresponding index set  $\mathcal{I}$  is typically limited, and the stabilizer  $\text{Stab}(\mathcal{I})$  remains nontrivial. Such constraints eliminate only those transformations that violate the specific statistical properties being enforced, leaving a family of admissible transformations that reflect intrinsic ambiguities of the separation model.

Crucially, the stabilizer  $\text{Stab}(\mathcal{I})$  is a *global* object: it characterizes residual ambiguities at the level of exact invariance under the observation map. While this global characterization is conceptually clear, it does not directly indicate how ambiguity reduction manifests under finite samples or small perturbations. This observation motivates the need for a complementary *local* characterization of stabilizer reduction, which is developed in the subsequent sections via Jacobian-based sensitivity analysis.

### B. Residual Ambiguities under Multiple Constraints

Even when observation statistics impose nontrivial constraints on the mixing model, residual ambiguities generally remain if only a single class of constraints is enforced. Such ambiguities correspond to nontrivial elements of the stabilizer  $\text{Stab}(\mathcal{I})$  associated with the chosen observation operators, and cannot be ruled out based on that information alone. These residual symmetries are not accidental; rather, they reflect intrinsic structural properties of the separation model under limited observational constraints.

When multiple classes of observation statistics are considered simultaneously, each class imposes a distinct invariance on the mixing model and therefore induces its own stabilizer. Let  $\mathcal{I}_1$  and  $\mathcal{I}_2$  denote index sets associated with two different families of observation operators. A transformation is compatible with both constraints if and only if it preserves both invariances. Accordingly, the admissible transformations under multiple constraints are characterized by the following elementary but structurally important relation.

*Lemma 1 (Intersection of stabilizers under multiple constraints):* Let  $\mathcal{I}_1$  and  $\mathcal{I}_2$  be index sets corresponding to two different families of observation operators. Then the stabilizer associated with their joint constraint satisfies

$$\text{Stab}(\mathcal{I}_1 \cup \mathcal{I}_2) = \text{Stab}(\mathcal{I}_1) \cap \text{Stab}(\mathcal{I}_2). \quad (13)$$

*Proof:* By definition of the stabilizer given in (10), a transformation belongs to  $\text{Stab}(\mathcal{I})$  if and only if it preserves every observation operator indexed by  $\mathcal{I}$ . Applying this definition to the union  $\mathcal{I}_1 \cup \mathcal{I}_2$ , a transformation belongs to  $\text{Stab}(\mathcal{I}_1 \cup \mathcal{I}_2)$  precisely when it preserves all operators in both families. This condition is equivalent to requiring membership in both  $\text{Stab}(\mathcal{I}_1)$  and  $\text{Stab}(\mathcal{I}_2)$ , which establishes (13). ■

The key point is that the benefit of combining multiple constraints does not depend on their specific algorithmic realization, but on how their induced stabilizers intersect at a structural level. Constraints derived from different sources of statistical information tend to eliminate complementary classes of symmetries, even when each constraint alone is insufficient for identifiability.

At the same time, the intersection relation in Lemma 1 remains a global statement. It specifies which transformations are ultimately excluded, but not how such exclusion manifests under finite perturbations or finite data. This observation motivates the introduction of a local perspective that can quantify stabilizer reduction in practice.

### C. Accumulation of Constraints and Structural Ambiguity Reduction

When multiple observation-induced constraints are enforced simultaneously, their effects accumulate through successive restrictions of the stabilizer. As additional constraint families are incorporated, the index set  $\mathcal{I}$  grows, and the stabilizer  $\text{Stab}(\mathcal{I})$  defined in (10) is progressively reduced through repeated intersections of the form (13). We refer to this progressive reduction of admissible transformations as *stabilizer shrinkage*.

From a global standpoint, stabilizer shrinkage reflects a systematic simplification of the symmetry inherent in the mixing model under limited observation. Each newly imposed class of observation statistics excludes transformations that were previously admissible, thereby reducing the degrees of freedom associated with residual ambiguity. This reduction is induced by the observation mechanism itself and should not be confused with numerical regularization or estimator-dependent effects.

In practical settings, different observation statistics restrict different subsets of the original continuous right-unitary freedom. As a consequence, distinct constraint families may lead to comparable ambiguity reductions even when their statistical origins differ. This explains why HOS-based and multi-SOS-based approaches, despite relying on different forms of statistical information, can exhibit structurally similar identifiability behavior.

To connect this global notion of ambiguity reduction to a local and tractable description, we explicitly exploit the fact that  $GL(n)$  is a Lie group and that  $\text{Stab}(\mathcal{I})$  forms a closed Lie subgroup, whose local structure is characterized by its associated Lie algebra (cf., e.g., [27]). As observation constraints accumulate, stabilizer shrinkage manifests not only as a set-theoretic reduction of admissible transformations, but also as a reduction in the dimension of the tangent space at the identity. From a dimensional perspective, this progressive reduction can be schematically expressed as

$$\dim T_I \text{Stab}(\mathcal{I}) \downarrow \text{ as constraints accumulate.} \quad (14)$$

This local reduction provides a direct measure of how strongly the observation statistics restrict infinitesimal right-unitary perturbations of the mixing matrix.

The tangent-space viewpoint naturally bridges global symmetry reduction and local sensitivity analysis. In particular, it motivates a Jacobian-based characterization of local identifiability, in which the sensitivity of the observation map to infinitesimal reparameterizations determines whether residual ambiguities persist locally. This perspective forms the basis of the Jacobian analysis developed in Section V.

Overall, this structural viewpoint clarifies when and how identifiability improves as additional observation statistics are incorporated. By framing ambiguity reduction in terms of stabilizer shrinkage and its manifestation in the tangent space, this section provides a coherent transition from global ambiguity analysis to the local identifiability results presented next.

## V. LOCAL IDENTIFIABILITY VIA JACOBIAN SENSITIVITY

### A. Local Perturbations and Constraint Sensitivity

Identifiability in blind source separation is often discussed as a global or asymptotic property. In practical settings with finite samples and imperfect statistical estimates, however, identifiability manifests through the local behavior of the model. It is therefore informative to examine how small perturbations of the mixing model affect the observation statistics enforced by a given set of constraints.

Let  $\text{Stab}(\mathcal{I})$  denote the stabilizer associated with a set of observation constraints, as defined in Section IV. Since  $GL(n)$  is a Lie group, admissible transformations in a neighborhood of the identity can be expressed through infinitesimal perturbations. After whitening, these reduce locally to right-orthogonal directions, motivating the use of skew-symmetric generators.

Specifically, we consider local perturbations of the form

$$H(\varepsilon) = H \exp(\varepsilon\Omega), \quad \Omega^\top = -\Omega, \quad (15)$$

where  $\varepsilon \in \mathbb{R}$  is a small scalar parameter and  $\Omega$  is a skew-symmetric matrix generating a local right action. This parameterization preserves orthogonality after whitening and provides a natural coordinate system for local analysis.

Under such perturbations, some directions  $\Omega$  induce noticeable changes in the observation statistics, while others leave them nearly unchanged. The former correspond to directions strongly constrained by the imposed statistics, whereas the latter indicate residual ambiguities that remain weakly constrained. Sensitivity to local perturbations therefore provides a natural lens through which the practical strength of observation-induced constraints can be assessed.

### B. Jacobian as a Numerical Probe of Residual Ambiguity

The local sensitivity of observation-induced constraints to infinitesimal perturbations can be examined through the Jacobian of the observation map  $\Phi$  defined in (7). The Jacobian with respect to the local perturbation (15) is defined as

$$J(H) = \left. \frac{\partial}{\partial \varepsilon} \Phi(H \exp(\varepsilon\Omega)) \right|_{\varepsilon=0}. \quad (16)$$

This Jacobian captures the first-order response of the observation constraints to infinitesimal transformations generated by  $\Omega$ . Locally, stabilizer shrinkage corresponds to a reduction of admissible tangent directions, and the Jacobian therefore indicates which perturbation directions remain compatible with the imposed constraints.

In practice, the Jacobian is used as a numerical probe of local constraint strength. Small Jacobian responses correspond to transformations that leave the statistics nearly invariant, indicating weakly constrained directions associated with residual ambiguities. Conversely, large responses indicate directions strongly restricted by the observation constraints.

For completeness, the formal definition of the Jacobian-based probe and its local parameterization are summarized in Appendix A.

### C. Relation to Structural Ambiguity Reduction

The numerical behavior revealed by Jacobian sensitivity corresponds directly to the structural ambiguity reduction discussed in Section IV. Observation-induced constraints restrict admissible transformations at the group level through stabilizer shrinkage, and this restriction appears locally through the behavior of the Jacobian.

Perturbation directions that remain weakly constrained by the imposed statistics correspond to tangent directions of the stabilizer  $\text{Stab}(\mathcal{I})$  at the identity. Here,  $T_I \text{Stab}(\mathcal{I})$  denotes the tangent space of the stabilizer  $\text{Stab}(\mathcal{I})$  at the identity element,

representing the space of infinitesimal admissible transformations. Such relationships between infinitesimal invariances and the tangent space of a symmetry group are standard in Lie theory (cf., e.g., [27]). When  $\text{Stab}(\mathcal{I})$  forms a regular Lie subgroup of  $\text{GL}(n)$ , its tangent space at the identity is naturally identified with the Lie algebra associated with the stabilizer, as expressed in (18).

At the level of first-order sensitivity, this relation can be summarized by

$$\ker J(H) \subseteq T_I \text{Stab}(\mathcal{I}), \quad (17)$$

indicating that locally unobservable perturbations align with infinitesimal stabilizer directions. Under the same regularity conditions, this inclusion tightens to  $\ker J(H) = T_I \text{Stab}(\mathcal{I})$ .

As additional constraints are accumulated, the stabilizer shrinks and its local tangent space decreases accordingly. Numerically, this reduction manifests as suppression of weakly sensitive directions in the Jacobian, reflected by the collapse of  $\ker J(H)$  and the growth of its smallest singular value.

## VI. UNIFYING NON-GAUSSIANITY AND OBSERVATION DIVERSITY

### A. Motivation

Classical blind source separation methods based on higher-order statistics (HOS) and those based on second-order statistics (SOS) are often treated as fundamentally different. However, from the structural viewpoint developed in Sections IV–V, both classes of methods reduce the same object: the residual ambiguity captured by the stabilizer of the observation constraints.

Let  $\mathcal{I}$  denote the index set of constraint operators associated with a given observation mechanism, and recall the definition of the stabilizer  $\text{Stab}(\mathcal{I})$  given in (10). Identifiability improves as this stabilizer shrinks under increasingly rich constraint families, regardless of how the constraints are instantiated.

From this perspective, the apparent dichotomy between HOS-based and SOS-based methods reflects different choices of the constraint index set  $\mathcal{I}$  rather than fundamentally distinct identifiability mechanisms. HOS-based methods correspond to constraint families  $\mathcal{I}_{\text{HOS}}$  induced by higher-order statistics, whereas SOS-based methods correspond to constraint families  $\mathcal{I}_{\text{SOS}}$  induced by observation diversity. A unified treatment therefore requires comparing how these different index sets reduce the same stabilizer, rather than comparing algorithms in isolation.

### B. Numerical Identifiability via Local Sensitivity

While the stabilizer  $\text{Stab}(\mathcal{I})$  provides a global characterization of residual ambiguity, its direct computation or comparison is generally intractable. As discussed in Section V, a local characterization is obtained by examining the Jacobian of the observation map.

Let  $J(H)$  denote the Jacobian defined in (16). The kernel  $\ker J(H)$  characterizes infinitesimal perturbations that remain

compatible with the imposed constraints and therefore provides a local representation of stabilizer shrinkage. In particular, under suitable regularity conditions,

$$\ker J(H) \cong \text{lie}(\text{Stab}(\mathcal{I})), \quad (18)$$

which links global symmetry reduction to local sensitivity. Here,  $\text{lie}(\text{Stab}(\mathcal{I}))$  denotes the Lie algebra associated with the stabilizer, that is, the space of infinitesimal generators of transformations that preserve the imposed observation constraints.

In practice, rather than using  $\ker J(H)$  as a binary identifiability criterion, we summarize local constraint strength through the smallest singular value  $\sigma_{\min}(J(H))$ , which measures how strongly stabilizer directions are suppressed. This quantity serves as a numerical probe of stabilizer shrinkage rather than as an estimator or optimality metric.

### C. Instantiating Stabilizer Shrinkage with HOS and SOS

The unifying interpretation becomes explicit when HOS-based and SOS-based constraints are examined within the same stabilizer framework. For HOS-based methods, the constraint family  $\mathcal{I}_{\text{HOS}}$  is determined by higher-order cumulant operators, whereas for SOS-based methods, the constraint family  $\mathcal{I}_{\text{SOS}}$  is determined by collections of second-order covariance operators.

Although  $\mathcal{I}_{\text{HOS}}$  and  $\mathcal{I}_{\text{SOS}}$  differ in their statistical origins, both act on the same object through stabilizer intersection:

$$\text{Stab}(\mathcal{I}_{\text{HOS}} \cup \mathcal{I}_{\text{SOS}}) = \text{Stab}(\mathcal{I}_{\text{HOS}}) \cap \text{Stab}(\mathcal{I}_{\text{SOS}}), \quad (19)$$

as established in (13). Consequently, identifiability improvements obtained by increasing non-Gaussianity or observation diversity correspond to different ways of shrinking the same stabilizer.

This formulation clarifies why non-Gaussianity and observation diversity can be viewed as alternative sources of constraint richness. Different constraint families reduce the same stabilizer through different mechanisms, while their effect on local identifiability is captured by the same Jacobian-based sensitivity. From a systems perspective, architectural choices (e.g., the number of lags or sensing diversity) and statistical assumptions influence identifiability only through the extent to which they reduce the dimension of the stabilizer, providing a structural guideline for the design of observation mechanisms in blind source separation.

## VII. NUMERICAL EXPERIMENTS

Throughout this section, we use the Jacobian-based probe  $\sigma_{\min}(J)$  as a diagnostic tool to visualize *structural ambiguity reduction* under different observation constraints. The absolute scale of the probe depends on the specific constraint family and is not intended for cross-experiment comparison or for ranking HOS- and SOS-based approaches. All experiments are designed to validate structural predictions derived from stabilizer shrinkage, rather than to benchmark separation algorithms.

### A. Experimental Setup and Evaluation Measures

We evaluate the structural effects discussed in Sections IV–V using controlled numerical experiments. The purpose of this section is *not* algorithm benchmarking or performance comparison, but to visualize how ambiguity reduction emerges through the accumulation of observation-induced constraints.

*a) Model and preprocessing.:* We consider a real-valued, linear instantaneous BSS model  $y = Hs$  with an equal number of sources and observations ( $n = m$ ). Unless otherwise stated, we set  $n = m = 3$  and whiten all mixtures using the sample covariance. After whitening, we select a reference mixing matrix  $H_0 = I$  as a canonical representative of the equivalence class discussed in Section II-A, and evaluate identifiability locally around this reference point. Accordingly, the remaining ambiguity corresponds to right-orthogonal transformations.

*b) Primary probe.:* Let  $\Phi(H)$  denote the collection of observation statistics introduced in Section II-C, evaluated under a given experimental configuration. Local sensitivity is probed using the right-orthogonal perturbation parameterization introduced in Section V-A (cf. (15)), together with the Jacobian defined in Section V-B (cf. (16)). In the present experiments, the Jacobian is evaluated at the reference point  $H_0 = I$ , and local sensitivity is assessed via infinitesimal perturbations around this point.

Our scalar diagnostic is defined as

$$\text{probe}(H_0) := \sigma_{\min}(J(H_0)), \quad (20)$$

which summarizes how strongly residual stabilizer directions are suppressed locally. All quantities are estimated from finite samples; we report Monte Carlo means and dispersion of  $\text{probe}(H_0)$ .

*c) Secondary index (sanity check only).:* As a secondary reference, we optionally report the Amari performance index (API) as a sanity check [22]. The API is not used to select algorithms or tune parameters; structural effects are assessed solely through the probe.

*d) Implementation.:* All experiments were implemented in Python using standard numerical libraries (NumPy/SciPy) and executed in a CPU-based environment. No GPU-specific operations or platform-dependent optimizations were used.

### B. Effect of Higher-Order Statistics (HOS)

Table I summarizes the simulation settings for the HOS-based experiments, including the choice of the reference mixing matrix  $H_0$  used for local sensitivity evaluation. These settings are chosen to isolate the effect of source non-Gaussianity on structural identifiability under higher-order constraints.

Sources are i.i.d. generalized Gaussian, where the shape parameter  $p$  controls deviation from Gaussianity, with the Gaussian boundary at  $p = 2.0$ . Higher-order information is incorporated through symmetric matrices derived from fourth-order cumulants, constructed using the standard JADE procedure.

The resulting behavior of the Jacobian-based probe evaluated at  $H_0$  is shown in Fig. 1. As predicted by the structural analysis, the probe collapses near the Gaussian boundary ( $p = 2.0$ ), consistent with the vanishing of fourth-order

TABLE I  
SIMULATION SETTINGS FOR THE HOS EXPERIMENT.

Number of sources/observations $n = m$	3
Sample length $T$	$1 \times 10^5$
Monte Carlo trials	50
Whitening	Yes
Reference mixing matrix	$H_0 = I$
Source distribution	Generalized Gaussian
Shape parameters $p$	{0.8, 1.0, 1.5, 2.0, 3.0}
HOS constraints	Fourth-order cumulant matrices

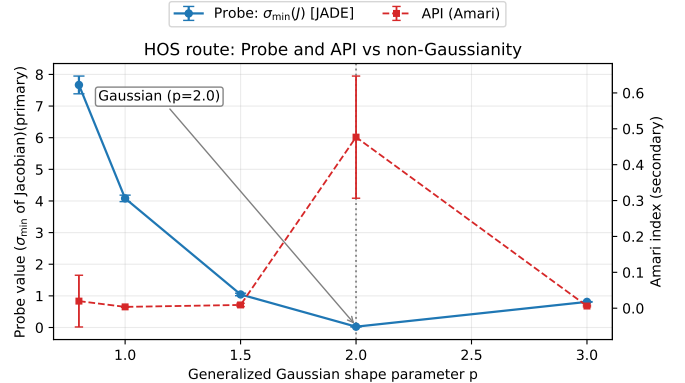


Fig. 1. Effect of source non-Gaussianity on structural identifiability in the HOS route. Primary axis: Jacobian-based probe  $\sigma_{\min}(J)$  computed from fourth-order cumulant constraints. The probe collapses near the Gaussian boundary ( $p = 2.0$ ) and increases for non-Gaussian sources. Secondary axis: Amari performance index (API). Error bars indicate Monte Carlo dispersion. Note that the absolute scales of both the primary probe and the secondary separation index are experiment-dependent and should not be compared across different figures or constraint families.

cumulants and the persistence of stabilizer directions under Gaussian sources. As  $p$  departs from 2.0, the probe increases, reflecting progressive activation of higher-order constraints and corresponding stabilizer shrinkage. The API is shown only as a sanity check and confirms degradation of separation quality in the Gaussian case.

### C. Effect of Observation Diversity via Multi-Lag SOS

We next examine ambiguity reduction driven by observation diversity using multi-lag second-order statistics, without relying on higher-order information. The corresponding simulation settings are summarized in Table II.

Sources are Gaussian AR(1) processes

$$s_i(t) = a_i s_i(t-1) + u_i(t), \quad u_i(t) \sim \mathcal{N}(0, 1),$$

with distinct coefficients  $(a_1, a_2, a_3) = (0.2, 0.6, 0.9)$ . Lagged covariance matrices of the whitened observations,

$$R_z(\tau) = \mathbb{E}[z(t)z(t-\tau)^\top], \quad \tau \in \mathcal{T}_L,$$

constitute the SOS constraints.

Figure 2 reports the resulting probe values evaluated at the reference mixing matrix  $H_0$  as a function of the number of lags  $L$ . For the minimal lag set ( $L = 1$ ), the probe remains small, indicating weak constraint strength. As additional lags are included ( $L > 1$ ), the probe increases overall, reflecting progressive suppression of residual stabilizer directions

TABLE II  
SIMULATION SETTINGS FOR THE SOS EXPERIMENT.

Number of sources/observations $n = m$	3
Sample length $T$	$1 \times 10^5$
Monte Carlo trials	50
Whitening	Yes
Reference mixing matrix	$H_0 = I$
Source model	Gaussian AR(1)
AR coefficients $(a_1, a_2, a_3)$	(0.2, 0.6, 0.9)
Lag set $\mathcal{T}_L$	$\{1, 2, \dots, L\}$
Lag count $L$	$\{1, 2, 3, 4, 5, 6, 7\}$
SOS constraints	Lagged covariance matrices

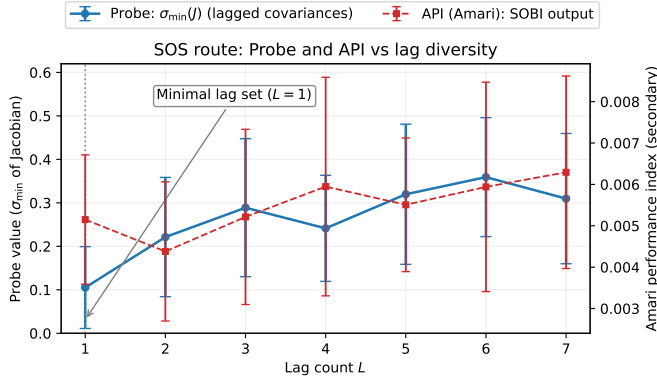


Fig. 2. Effect of observation diversity on structural identifiability in the SOS route. Primary axis: Jacobian-based probe  $\sigma_{\min}(J)$  for lag counts  $L = 1, 2, \dots, 7$ . Secondary axis: Amari performance index (API). Increasing lag diversity strengthens the probe, while gains saturate for larger  $L$ . Note that the absolute scales of both the primary probe and the secondary separation index are experiment-dependent and should not be compared across different figures or constraint families.

through accumulated temporal constraints. For larger  $L$ , gains diminish due to finite-sample effects. The API remains nearly constant, indicating that separation quality is already saturated, while structural ambiguity continues to shrink.

#### D. Trade-off Between Source Statistics and Observation Diversity

Finally, we visualize the trade-off between source statistics and observation diversity using second-order observation constraints, without explicitly combining higher-order statistics. Here, the shape parameter  $p$  characterizes the source process only and does not enter the SOS constraint operators themselves; the probe  $\text{probe}_{\text{SOS}}$  is computed exclusively from second-order (lagged covariance) operators, while varying  $p$  modifies the effective second-order structure available after whitening. For each  $(p, L)$ , we evaluate the Jacobian-based probe defined in (20) for the SOS constraint family:

$$\text{probe}_{\text{SOS}}(p, L) := \sigma_{\min}(J_{\text{SOS}}(H_0)). \quad (21)$$

Based on this quantity, we define the minimal lag count required to reach a target sensitivity level  $\varepsilon$  as

$$L_{\min}(p; \varepsilon) := \min\{L : \text{probe}_{\text{SOS}}(p, L) \geq \varepsilon\}. \quad (22)$$

The resulting trade-off is summarized in Fig. 3. Near the Gaussian boundary, where statistical structure is weak, larger lag diversity is required to reach the same probe level.

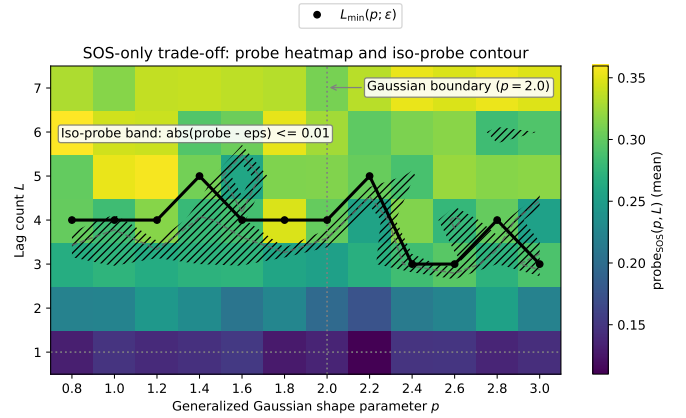


Fig. 3. Trade-off between source statistics and observation diversity under second-order observation constraints. Heatmap:  $\text{probe}_{\text{SOS}}(p, L)$ . Markers:  $L_{\min}(p; \varepsilon)$  defined in (22). This visualization highlights structurally equivalent configurations rather than performance optima.

Away from this boundary, fewer lags suffice. Different pairs  $(p, L)$  that yield the same probe value therefore correspond to structurally equivalent configurations in terms of local identifiability, illustrating how non-Gaussianity and observation diversity contribute comparably to stabilizer shrinkage.

## VIII. CONCLUSION

This paper examined identifiability in blind source separation (BSS) from a structural standpoint, focusing on how observation-induced constraints eliminate symmetry-induced ambiguities. HOS-based and SOS-based approaches were characterized as mechanisms that restrict the class of transformations consistent with the observed data. Within this formulation, identifiability is governed by the extent to which statistical constraints shrink residual ambiguities, and the classical distinction between HOS and SOS is attributed to the origin of the imposed constraints.

To connect this structural characterization with finite-sample behavior, we introduced a Jacobian-based sensitivity probe as a numerical diagnostic of local identifiability. Numerical experiments confirmed the structural interpretation: in the HOS route, the probe collapses near the Gaussian limit and increases with stronger non-Gaussian constraints; in the SOS route, increasing lag diversity strengthens the probe even under Gaussian sources; and their trade-off can be visualized within a common structural scale. These results provide a local characterization of residual ambiguities through the kernel and sensitivity of the Jacobian.

Beyond individual mechanisms, the main contribution of this work is a constraint-centered reorganization of identifiability. By separating structural effects from algorithmic implementations, the proposed view clarifies why methods with different formulations often exhibit similar empirical behavior and why additional constraints can improve robustness even when conventional performance indices saturate. From a circuits-and-systems perspective, observation architecture choices (e.g., lag diversity) and statistical assumptions influence identifiability through their effect on stabilizer reduction

under finite-sample and computational constraints. In this sense, identifiability can be viewed as the collapse of an infinite equivalence class to a finite residual ambiguity under observation-induced constraints (cf. Sections II-C and IV-C).

Several extensions naturally follow. The same structural analysis applies to complex-valued formulations and to broader observation models, including convolutive and block or oversampled settings, as well as to multi-way representations arising in tensor-based formulations [28]. The Jacobian-based probe also supports a design-oriented evaluation of constraint configurations based on their ambiguity-suppressing effect. More generally, the proposed interpretation provides a basis for extending constraint-induced ambiguity reduction to other blind inference problems beyond classical BSS.

Overall, by organizing identifiability around constraint-induced ambiguity reduction, this work clarifies the operating principles of classical BSS methods and provides a concise structural basis for the design and evaluation of future blind separation approaches.

## APPENDIX A

### FORMAL DEFINITION OF THE JACOBIAN-BASED PROBE

#### A. Observation Relations and Parameterization

This appendix formalizes the Jacobian-based probe used in Sections V and VII. All models, assumptions, and notation are identical to those introduced in Section II, and the local perturbation model follows Section V. The purpose here is purely notational: to state the probe definition used in the numerical evaluations, without introducing additional theoretical claims.

Let  $\Phi(H)$  denote the observation map defined in (7), whose components depend on the chosen constraint family (e.g., HOS or multi-SOS). Throughout, local sensitivity is evaluated under right-orthogonal reparameterizations as in (15).

#### B. Jacobian of Observation Relations

Consider the local perturbation  $H(\theta) = H \exp(\theta\Omega)$  with  $\Omega^\top = -\Omega$  as in (15). The Jacobian of the observation map along this perturbation is defined by

$$J(H) = \left. \frac{\partial}{\partial \theta} \Phi(H \exp(\theta\Omega)) \right|_{\theta=0}, \quad (23)$$

which coincides with the definition used in (16). The Jacobian provides a first-order linearization of how the enforced observation statistics respond to infinitesimal right-orthogonal perturbations.

It is emphasized that  $J(H)$  is used only as a local sensitivity probe. It is not associated with an estimator, likelihood function, or statistical optimality criterion, and is introduced solely to quantify how strongly the imposed observation constraints respond to parameter perturbations.

*Concrete instantiations of  $\Phi(H)$ .*: The abstract observation map  $\Phi(H)$  specializes to concrete forms depending on the constraint family. For HOS-based constraints,

$$\Phi_{\text{HOS}}(H) = \{C_k^{(4)}(H)\}_{k=1}^K, \quad (24)$$

where  $C_k^{(4)}(H)$  denote symmetric matrices constructed from fourth-order cumulants (e.g., as in the JADE construction). For SOS-based constraints with lag set  $\mathcal{T}_L = \{1, \dots, L\}$ ,

$$\Phi_{\text{SOS}}(H) = \{R_z(\tau) \mid \tau \in \mathcal{T}_L\}, \quad R_z(\tau) = \mathbb{E}[z(t)z(t-\tau)^\top]. \quad (25)$$

In both cases, we write  $\Phi(H) = \{A_i(H)\}_{i \in \mathcal{I}}$  where  $A_i(H)$  denotes the  $i$ -th matrix-valued component of the observation map (e.g.,  $A_i(H) = C_k^{(4)}(H)$  for HOS-based constraints or  $A_i(H) = R_z(\tau)$  for SOS-based constraints). For local sensitivity analysis, we use the stacked vector representation  $\phi(H)$  obtained by vectorizing and concatenating these components:

$$\phi(H) = \begin{bmatrix} \text{vec } A_1(H) \\ \vdots \\ \text{vec } A_{|\mathcal{I}|}(H) \end{bmatrix} \in \mathbb{R}^{|\mathcal{I}|n^2}, \quad (26)$$

where  $\text{vec}(\cdot)$  denotes the standard column-wise vectorization of a matrix. The Jacobian  $J(H) \in \mathbb{R}^{(|\mathcal{I}|n^2) \times d}$  with  $d = n(n-1)/2$  is then obtained by collecting directional derivatives of  $\phi(H)$  with respect to infinitesimal right-orthogonal perturbations of  $H$ , parameterized by a basis of skew-symmetric generators  $\Omega$ .

#### C. Definition and Interpretation of the Probe

The Jacobian-based probe is defined as

$$\text{probe}(H) := \sigma_{\min}(J(H)), \quad (27)$$

where  $\sigma_{\min}(\cdot)$  denotes the smallest singular value. Small values of  $\text{probe}(H)$  indicate the presence of perturbation directions that leave the enforced statistics nearly unchanged, whereas larger values indicate stronger suppression of such weakly observable directions. This interpretation is consistent with the structural viewpoint in Section IV and the local analysis in Section V.

Importantly, the probe does not define identifiability in a strict sense, nor does it characterize the full symmetry structure of the model. It is used in Section VII only as a diagnostic tool to visualize and compare the effects of different constraint configurations, without introducing new identifiability criteria.

#### D. Practical Computation from Sample Statistics

In experiments, the statistics entering  $\Phi(H)$  are estimated from finite data samples. Accordingly,  $J(H)$  and  $\text{probe}(H)$  are computed using sample-based estimates, and the reported values reflect both the imposed structural constraints and estimation variability. All numerical results in Section VII are therefore averaged over Monte Carlo trials and accompanied by dispersion measures.

## APPENDIX B

### SITUATIONS IN WHICH IDENTIFIABILITY CONSTRAINTS DO NOT SHRINK THE STABILIZER

This appendix provides explicit examples that support the asymmetry stated in Section II-C (Remark on identifiability): “richness” alone does not shrink the stabilizer unless constraints act at the appropriate level. All notation and assumptions follow Section II and Section II-C, and we focus only on the transformations that preserve the available observations.

### A. Output Non-Gaussianity Alone Is Insufficient

Assume that only the output distribution  $P_y$  is observed, while no constraint is imposed on the source distribution  $P_s$ . Then the right-unitary reparameterization

$$H \mapsto HU, \quad U \in \mathcal{U}(n), \quad (28)$$

cannot be excluded from  $P_y$  alone. Indeed, defining  $s' = U^*s$  yields the equivalent factorization

$$y = Hs = (HU)s', \quad (29)$$

so the same  $P_y$  is compatible with an entire right-unitary orbit of mixing matrices. Hence, output non-Gaussianity by itself does not restrict the stabilizer of the mixing model.

### B. Input-Side Structural Diversity Without Source Constraints Is Also Insufficient

Assume that the source process is Gaussian but exhibits rich second-order structure (e.g., nontrivial multi-lag covariances, oversampled/block covariances, or cyclostationary second-order statistics). Without additional source-side constraints that fix a preferred representation, the same right-unitary reparameterization persists:

$$s'(t) = U^*s(t), \quad H' = HU, \quad U \in \mathcal{U}(n). \quad (30)$$

Gaussianity is preserved under unitary transformations, and second-order structure transforms by unitary congruence; for example,

$$\Sigma_{s'}(\tau) := \mathbb{E}[s'(t)s'^*(t-\tau)] = U^*\Sigma_s(\tau)U. \quad (31)$$

Thus, input-side second-order “richness” alone does not shrink the stabilizer unless additional constraints anchor the source representation.

### C. Failure of Single-Lag SOS

This subsection presents a minimal counterexample that isolates the limitation of a single *output-side* second-order constraint and clarifies why observation diversity is essential for stabilizer shrinkage. All notation and assumptions follow Sections II–II-C, and we focus exclusively on the effect of lagged covariance operators.

Accordingly, when only the single-lag covariance operator is enforced, the stabilizer remains the full unitary group,

$$\text{Stab}(H; \text{Cov}(0)) = \mathcal{U}(n), \quad (32)$$

and the corresponding Jacobian kernel is nontrivial,

$$\ker J(H) \neq \{0\}, \quad (33)$$

where  $J(H)$  denotes the Jacobian of the observation map defined in (16). This demonstrates that a single second-order constraint does not reduce the continuous right-unitary ambiguity: infinitesimal right-unitary perturbations remain locally invisible to the enforced statistics.

Now consider the addition of a second lag  $\tau \neq 0$ , yielding the pair of operators  $\{\Sigma_y(0), \Sigma_y(\tau)\}$ . Under generic

conditions—specifically, when the joint spectrum of the associated source covariance operators is simple—the joint commutant of these operators is finite. In this case, the stabilizer collapses to a finite set, and the local ambiguity vanishes:

$$\ker J(H) = \{0\}. \quad (34)$$

Thus, the inclusion of a second lag is sufficient to eliminate the continuous right-unitary freedom that persists under a single-lag constraint.

This example highlights the minimal nature of stabilizer shrinkage under *output-side* second-order statistics: observation diversity must be sufficient to break the relevant symmetry. Single-lag SOS fails to do so, while multi-lag SOS succeeds precisely by inducing a finite stabilizer through joint constraints.

### D. Interpretation

The above examples support the central message of the paper: identifiability in BSS emerges only when constraints restrict the admissible transformations of the mixing model at the appropriate level. In particular, stabilizer shrinkage requires either (i) source-side constraints that fix a preferred representation (e.g., non-Gaussianity combined with independence), or (ii) output-side operator diversity that effectively constrains the right-unitary action (e.g., multi-lag/oversampled covariance operators whose joint commutant is finite). By contrast, statistical or structural “richness” by itself does not shrink the stabilizer unless anchored by such constraints.

### E. HOS Trade-off Visualization

For completeness, we provide an additional trade-off visualization for the HOS route. We construct a family of fourth-order cumulant matrices  $\{C_i\}$  (JADE-style) from whitened mixtures and evaluate the Jacobian-based probe at  $H = I$ . Let  $K$  denote the number of cumulant matrices used as constraints (sorted by Frobenius norm), and define

$$\text{probe}_{\text{HOS}}(p, K) = \sigma_{\min}(J_{\text{HOS}}).$$

Figure 4 shows a heatmap of  $\log_{10} \text{probe}_{\text{HOS}}(p, K)$ , together with the design-oriented summary

$$K_{\min}(p; \varepsilon) := \min\{K : \text{probe}_{\text{HOS}}(p, K) \geq \varepsilon\},$$

where  $\varepsilon = 0.5$ .

As expected, the HOS probe collapses rapidly near the Gaussian boundary ( $p = 2$ ) across all  $K$ , reflecting the disappearance of fourth-order information for Gaussian sources. Away from the boundary, increasing  $K$  strengthens the probe, and only a small number of HOS constraints may suffice to exceed the target level. The hatched region indicates an iso-probe band

$$|\text{probe}_{\text{HOS}}(p, K) - \varepsilon| \leq \delta$$

(with  $\delta = 0.05$ ), serving as a reading aid rather than a sharp boundary.

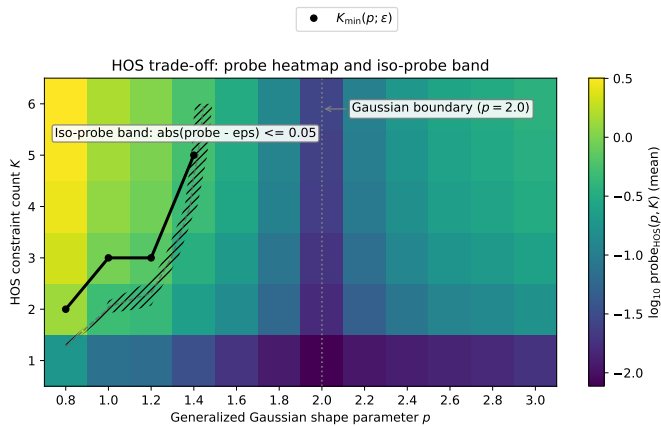


Fig. 4. HOS trade-off visualization. Heatmap:  $\log_{10} \text{probe}_{\text{HOS}}(p, K)$  (Monte Carlo mean) as a function of generalized Gaussian shape parameter  $p$  and the number  $K$  of cumulant-matrix constraints (JADE-style, sorted by Frobenius norm). Black markers and solid line:  $K_{\min}(p; \epsilon)$  with  $\epsilon = 0.5$ . Hatched region: iso-probe band  $|\text{probe}_{\text{HOS}} - \epsilon| \leq \delta$  with  $\delta = 0.05$  (reading aid; not a sharp boundary). The vertical dotted line marks the Gaussian boundary ( $p = 2.0$ ).

## APPENDIX C

### REMARKS ON CLASSICAL ALGORITHMS (ARXIV VERSION)

#### A. AMUSE and FastICA

Algorithms such as AMUSE and FastICA are often described as SOS- or HOS-based methods. From the viewpoint of identifiability, AMUSE relies on a single nonzero-lag covariance and therefore corresponds to the minimal SOS configuration ( $L = 1$ ), while FastICA exploits higher-order information through an implicit optimization criterion. In both cases, the set of identifiable transformations is determined by the statistics being enforced; the algorithms themselves primarily affect estimation accuracy under finite samples rather than the underlying structural identifiability.

## REFERENCES

- [1] E. Kofidis, “Blind Source Separation: Fundamentals and Recent Advances (A Tutorial Overview Presented at SBrT-2001),” Mar. 2016, arXiv:1603.03089 [stat] version: 1. [Online]. Available: <http://arxiv.org/abs/1603.03089>
- [2] L. Tong, R.-w. Liu, V. Soon, and Y.-F. Huang, “Indeterminacy and identifiability of blind identification,” *IEEE Transactions on Circuits and Systems*, vol. 38, no. 5, pp. 499–509, May 1991. [Online]. Available: <https://ieeexplore.ieee.org/document/76486>
- [3] P. Comon, “Independent component analysis, A new concept?” *Signal Processing*, vol. 36, no. 3, pp. 287–314, Apr. 1994. [Online]. Available: <https://www.sciencedirect.com/science/article/pii/0165168494900299>
- [4] A. Hyvärinen and E. Oja, “Independent component analysis: algorithms and applications,” *Neural Networks*, vol. 13, no. 4, pp. 411–430, Jun. 2000. [Online]. Available: <https://www.sciencedirect.com/science/article/pii/S0893608000000265>
- [5] A. Belouchrani, K. Abed-Meraim, J.-F. Cardoso, and E. Moulines, “A blind source separation technique using second-order statistics,” *IEEE Transactions on Signal Processing*, vol. 45, no. 2, pp. 434–444, Feb. 1997. [Online]. Available: <http://ieeexplore.ieee.org/document/554307/>
- [6] L. Tong, V. Soon, Y. Huang, and R. Liu, “AMUSE: a new blind identification algorithm,” *IEEE International Symposium on Circuits and Systems*, pp. 1784–1787, 1990, conference Name: IEEE International Symposium on Circuits and Systems Place: New Orleans, LA, USA Publisher: IEEE. [Online]. Available: <http://ieeexplore.ieee.org/document/111981/>
- [7] P. Comon and C. Jutten, “Handbook of blind source separation: Independent component analysis and applications,” *Academic Press*, 2010.
- [8] A. Aïssa-El-Bey, K. Abed-Meraim, Y. Grenier, and Y. Hua, “A general framework for second-order blind separation of stationary colored sources,” *Signal Processing*, vol. 88, no. 9, pp. 2123–2137, Sep. 2008. [Online]. Available: <https://www.sciencedirect.com/science/article/pii/S0165168408001114>
- [9] B. Kivva, G. Rajendran, P. Ravikumar, and B. Aragam, “Identifiability of deep generative models without auxiliary information,” Oct. 2022, arXiv:2206.10044 [cs]. [Online]. Available: <http://arxiv.org/abs/2206.10044>
- [10] K. Helwani, M. Togami, P. Smaragdis, and M. M. Goodwin, “Sound Source Separation Using Latent Variational Block-Wise Disentanglement,” Feb. 2024, arXiv:2402.06683 [eess]. [Online]. Available: <http://arxiv.org/abs/2402.06683>
- [11] D. Mika and J. Jozwik, “Lie Group Methods in Blind Signal Processing,” *Sensors*, vol. 20, no. 2, p. 440, Jan. 2020, publisher: Multidisciplinary Digital Publishing Institute. [Online]. Available: <https://www.mdpi.com/1424-8220/20/2/440>
- [12] M. Pedersen, J. Larsen, U. Kjems, and L. Parra, “A SURVEY OF CONVOLUTIONAL BLIND SOURCE SEPARATION METHODS,” Technical University of Denmark, Tech. Rep., 2007.
- [13] M. Congedo, C. Gouy-Pailler, and C. Jutten, “On the blind source separation of human electroencephalogram by approximate joint diagonalization of second order statistics,” *Clinical Neurophysiology*, vol. 119, no. 12, pp. 2677–2686, Dec. 2008. [Online]. Available: <https://www.sciencedirect.com/science/article/pii/S1388245708009668>
- [14] A. Benveniste, M. Goursat, and G. Ruget, “Robust identification of a nonminimum phase system: Blind adjustment of a linear equalizer in data communications,” *IEEE Transactions on Automatic Control*, vol. 25, no. 3, pp. 385–399, Jun. 1980. [Online]. Available: <https://ieeexplore.ieee.org/document/1102343>
- [15] R. Bellman and K. J. Åström, “On structural identifiability,” *Mathematical Biosciences*, vol. 7, no. 3, pp. 329–339, Apr. 1970. [Online]. Available: <https://www.sciencedirect.com/science/article/pii/002555647090132X>
- [16] J. Cardoso and A. Souloumiac, “Blind beamforming for non-gaussian signals,” *IEE Proceedings F Radar and Signal Processing*, vol. 140, no. 6, p. 362, 1993. [Online]. Available: <https://digital-library.theiet.org/content/journals/10.1049/ip-f-2.1993.0054>
- [17] E. Moulines, P. Duhamel, J.-F. Cardoso, and S. Mayrargue, “Subspace methods for the blind identification of multichannel FIR filters,” *IEEE Transactions on Signal Processing*, vol. 43, no. 2, pp. 516–525, Feb. 1995. [Online]. Available: <https://ieeexplore.ieee.org/document/348133>
- [18] L. Tong, G. Xu, and T. Kailath, “Blind identification and equalization based on second-order statistics: a time domain approach,” *IEEE Transactions on Information Theory*, vol. 40, no. 2, pp. 340–349, Mar. 1994. [Online]. Available: <https://ieeexplore.ieee.org/document/312157>
- [19] I. N. Herstein, *Abstract Algebra*, 3rd ed. New York: John Wiley & Sons, 1996.
- [20] W. Naanaa and J.-M. Nuzillard, “A geometric approach to blind separation of nonnegative and dependent source signals,” *Signal Processing*, vol. 92, no. 11, pp. 2775–2784, Nov. 2012. [Online]. Available: <https://www.sciencedirect.com/science/article/pii/S0165168412001648>
- [21] X.-F. Gong, Q.-H. Lin, F.-Y. Cong, and L. D. Lathauwer, “Double Coupled Canonical Polyadic Decomposition for Joint Blind Source Separation,” Jul. 2018, arXiv:1612.09466 [stat]. [Online]. Available: <http://arxiv.org/abs/1612.09466>
- [22] S. Amari, A. Cichocki, and H. Yang, “A New Learning Algorithm for Blind Signal Separation,” in *Advances in Neural Information Processing Systems 8*. MIT Press, 1995, pp. 757–763.
- [23] “Handbook of Blind Source Separation,” ISBN: 9780123747266. [Online]. Available: <https://www.sciencedirect.com/book/edited-volume/9780123747266/handbook-of-blind-source-separation>
- [24] O. Shalvi and E. Weinstein, “New criteria for blind deconvolution of nonminimum phase systems (channels),” *IEEE Transactions on Information Theory*, vol. 36, no. 2, pp. 312–321, Mar. 1990. [Online]. Available: <https://ieeexplore.ieee.org/document/52478>
- [25] J.-F. Cardoso, “High-Order Contrasts for Independent Component Analysis,” *Neural Computation*, vol. 11, no. 1, pp. 157–192, Jan. 1999. [Online]. Available: <https://direct.mit.edu/neco/article/11/1/157-192/6234>
- [26] L. Tong, G. Xu, and T. Kailath, “A new approach to blind identification and equalization of multipath channels,” in [1991] *Conference Record of the Twenty-Fifth Asilomar Conference on Signals, Systems & Computers*, Nov. 1991, pp. 856–860 vol.2, ISSN: 1058-6393. [Online]. Available: <https://ieeexplore.ieee.org/document/186568>

- [27] B. C. Hall, *Lie Groups, Lie Algebras, and Representations: An Elementary Introduction*, 2nd ed., ser. Graduate Texts in Mathematics. Cham: Springer, 2015, vol. 222.
- [28] T. T. Le, K. Abed-Meraim, P. Ravier, O. Buttelli, and A. Holobar, "Tensor decomposition meets blind source separation," *Signal Processing*, vol. 221, p. 109483, Aug. 2024. [Online]. Available: <https://www.sciencedirect.com/science/article/pii/S0165168424001026>